Int. J. Electrochem. Sci., 2 (**2007**) 386 - 405

International Journal of ELECTROCHEMICAL SCIENCE
www.electrochemsci.org

Comparison Between Derivative and Differential Pulse Voltammetric Curves of EC, CE and Catalytic Processes at Spherical Electrodes and Microelectrodes

A. Molina[*] *and I. Morales*

Departamento de Química Física, Universidad de Murcia, Espinardo 30100, Murcia, Spain
[*]E-mail: amolina@um.es

Received: 5 February 2007 / *Accepted:* 18 April 2007 / *Published:* 1 May 2007

Analytical expressions for derivative voltammetry (DV) and differential pulse voltammetry (DPV) corresponding to EC, CE and catalytic mechanisms at spherical electrodes are deduced. Through comparison of these responses, criteria to discriminate between these three mechanisms are established. Methods for determining the kinetic constants of the chemical reactions based on the measurement of peak coordinates are also proposed.

Keywords: Homogeneous kinetic; Steady state; Spherical electrodes; Microelectrodes; Differential pulse voltammetry.

1. INTRODUCTION

In previous papers we have tackled catalytic and CE mechanisms in voltammetry with constant potential at spherical electrodes under kinetic steady state conditions and also supposing a purely diffusive behaviour for pseudo-species ζ ($c_B + c_C$) and for species c_D [1-3]. This last approximation has been introduced by us [2, 3], leading to simple equations which have been shown to be valid for any electrode radius (if the kinetic is fast enough) or for any value of the kinetic constants of the chemical reaction (when the electrode radius is less than a certain value) [2, 3]. In all the mechanisms we have considered that all the species participating in the processes are initially present in the solution.

In this paper we have deduced first the response obtained for an EC mechanism in potential constant voltammetry in order to compare the expressions of the $I-E-t$ curves of the three mechanisms. Afterwards, we obtain the corresponding responses to the EC, CE and catalytic mechanisms when derivative voltammetry (DV) and/or differential pulse voltammetry (DPV) are used,

since, as is demonstrated in this paper, under the right conditions, the expressions of the derivative voltammetric response can be used in differential pulse voltammetry (as occurs for a reversible E process) if a sufficiently small potential step ΔE is used [4-8].

The use of the above techniques with spherical electrodes or microelectrodes allows us to distinguish clearly between EC, CE and catalytic processes and also to propose methods to determine the kinetic parameters of the chemical steps, from the measurement of the height and position of the observed peaks. We also demonstrate that under the above conditions [2, 3] the $I-E$ curves corresponding to EC, CE and catalytic mechanisms can be written in a formally identical way to those for an E mechanism where the half wave potential $E_{1/2}$ for each process is dependent on the homogeneous kinetic rate constants in the case of EC and CE mechanisms, but coincides with $E^{0'}$ in the catalytic mechanism. This $I-E$ behaviour gives rise to the peak parameters of DV and DPV corresponding to the three above mechanisms having an analogous form to that corresponding to the E mechanism, referring to the suitable $E_{1/2}$.

2. KINETIC STEADY STATE APPROXIMATION SUPPOSING A PURELY DIFFUSIVE BEHAVIOUR FOR ζ AND c_A OR c_D

We will simultaneously analyse the following three reaction schemes [4, 9]:

$$A + ne^- \rightleftharpoons B \underset{k_2}{\overset{k_1}{\rightleftharpoons}} C \qquad \text{EC mechanism (I)}$$

$$B \underset{k_2}{\overset{k_1}{\rightleftharpoons}} C + ne^- \rightleftharpoons D \qquad \text{CE mechanism (II)}$$

$$\left.\begin{array}{l} B \underset{k_2}{\overset{k_1}{\rightleftharpoons}} C + ne^- \rightleftharpoons B \\ C + ne^- \rightleftharpoons B \underset{k_2}{\overset{k_1}{\rightleftharpoons}} C \end{array}\right\} \qquad \text{Catalytic mechanism (III)}$$

Schemes (I) and (II) correspond to first or pseudo-fist order EC and CE mechanisms in which only one of the species participating in the electrode process (the reduced one, B, in the EC process, or the oxidized one, C, in the CE process) is chemically coupled to different species. Moreover, a catalytic process is represented by Scheme (III).

For these three mechanisms we define the equilibrium constant *K*:

$$K = \frac{k_2}{k_1} = \frac{c_B^*}{c_C^*} \qquad (1)$$

and

$$\kappa = k_1 + k_2 \qquad (2)$$

c_i^* (*i*=B or C) being the bulk concentrations of species B and C and k_1 and k_2 the homogeneous reaction rate constants.

If we consider the kinetic steady state approximation supposing a purely diffusive behaviour for pseudo-species ζ and species c_A (EC mechanism) or c_D (CE mechanism) [2, 3], the following expressions for the $I-E-t$ curves are obtained for these three mechanisms, when considering identical diffusion coefficients:

2.1. EC mechanism

For an EC process this approximation [2, 3] supposes an intermediate situation between the kinetic steady state (whose equations can be obtained following the procedure indicated in Ref. [3]) and the "true" steady state [10]. Therefore, under these conditions (see Refs. [2, 3]) and supposing that all species participating in Scheme I (A, B and C) are initially present in the solution, we obtain the following expression for the $I-E-t$ curve in the case of EC process (see Appendix):

$$\frac{I^{EC}}{I_d\left(c_A^*\right)}=\frac{\left(1+K\right)-Ke^{\eta}\,\zeta^*/c_A^*}{1+K+e^{\eta}\left(K+\delta_r/\delta\right)} \tag{3}$$

being

$$I_d\left(c_A^*\right)=nFADc_A^*/\delta \tag{4}$$

$$\zeta^*=c_B^*+c_C^* \tag{5}$$

$$\eta=\frac{nF}{RT}\left(E-E^{0'}\right) \tag{6}$$

δ_r and δ are the reaction and diffusion layer thicknesses for a spherical electrode [2], respectively, which have been shown to be independent of the applied potential [3], given by:

$$\delta_r=\left(\frac{1}{r_0}+\sqrt{\frac{\kappa}{D}}\right)^{-1}=\frac{r_0\sqrt{D}}{\sqrt{D}+r_0\sqrt{\kappa}} \tag{7}$$

$$\delta=\left(\frac{1}{r_0}+\frac{1}{\sqrt{\pi Dt}}\right)^{-1}=\frac{r_0\sqrt{\pi Dt}}{r_0+\sqrt{\pi Dt}} \tag{8}$$

2.2. CE mechanism

As in the case of the EC process, this approximation [2, 3] leads to a handy, time dependent expression for the $I-E-t$ curve, supposing that all species participating in Scheme II (B, C and D) are initially present in the solution:

$$\frac{I^{CE}}{I_d\left(\zeta^*\right)}=\frac{1-\left(1+K\right)e^{\eta}\,c_D^*/\zeta^*}{1+\left(1+K\right)e^{\eta}+K\,\delta_r/\delta} \tag{9}$$

where

$$I_d\left(\zeta^*\right) = nFAD\zeta^*/\delta \tag{10}$$

Note that Eq. (9) can be obtained from Eq. (3) corresponding to an EC process replacing K, η and *n* by $1/K$, $-\eta$ and -*n*, respectively, and taking into account that $c_{\mathrm{A}}^* \equiv c_{\mathrm{D}}^*$.

2.3. Catalytic mechanism

In the case of the catalytic mechanism (for which $\zeta = c_{\mathrm{B}} + c_{\mathrm{C}} = \zeta^* = c_{\mathrm{B}}^* + c_{\mathrm{C}}^* = \mathrm{ctn}$), and due to the singularities that this mechanism shows in its route to the steady state [1], the supposition of a purely diffusive behaviour does not have an additional meaning regarding the kinetic steady state since both assumptions lead to the same time independent response, in contrast to the cases of EC and CE mechanisms:

$$\frac{I^{\mathrm{cat}}}{nFAD\zeta^*} = \frac{1}{\delta_r}\frac{1-Ke^{\eta}}{(1+K)\left(1+e^{\eta}\right)} \tag{11}$$

2.4. Comparison between EC, CE, catalytic and E processes

It is very interesting to highlight that the simplified equations for the current corresponding to EC and CE mechanisms (Eqs. (3) and (9), respectively) present two interesting limit physical situations. Indeed, if we suppose that the diffusion layer thickness δ turns into the reaction layer thickness δ_r, the kinetic plays its maximum role and the responses obtained for EC or CE [2, 3] mechanisms (Eqs. (3) and (9), respectively), by making $c_{\mathrm{A}}^* = c_{\mathrm{C}}^*$ in Eq. (3) or $c_{\mathrm{D}}^* = c_{\mathrm{B}}^*$ in Eq. (9), convert into that corresponding to a catalytic mechanism [1] (Eq. (11)), i.e.,

$$I^{\mathrm{EC}}_{c_{\mathrm{A}}^*=c_{\mathrm{C}}^*} = I^{\mathrm{CE}}_{c_{\mathrm{D}}^*=c_{\mathrm{B}}^*} = I^{\mathrm{cat}} \quad \text{if} \quad \delta \to \delta_r \tag{12}$$

On the other hand, if we suppose that the reaction layer thickness δ_r reaches the value of the diffusion layer thickness δ, Eqs. (3), (9) and (11) obtained for EC, CE and catalytic mechanisms, respectively, become that corresponding to the simple charge transfer process $\mathrm{A} + ne^- \rightleftarrows \mathrm{B}$ (for EC mechanism) or $\mathrm{C} + ne^- \rightleftarrows \mathrm{D}$ (for CE and catalytic mechanisms), i.e.,

$$\left.\begin{aligned} I^{\mathrm{EC}} &\to I^{\mathrm{E}}\left(\mathrm{A} + ne^- \rightleftarrows \mathrm{B}\right) \\ I^{\mathrm{CE}} &\to I^{\mathrm{E}}\left(\mathrm{C} + ne^- \rightleftarrows \mathrm{D}\right) \\ I^{\mathrm{cat}} &\to I^{\mathrm{E}}\left(\mathrm{C} + ne^- \rightleftarrows \mathrm{D}\right) \end{aligned}\right\} \quad \text{if} \quad \delta_r \to \delta \tag{13}$$

The main achievement of these expressions for EC, CE and catalytic processes, which are applicable for $\kappa t \geq 9.7$ and/or $\sqrt{Dt}/r_0 \geq 0.63$ [3], is that the responses can be linearized in a formally identical way to that corresponding to an E reversible process, in such a way that, even if all the species are initially present in the solution, they fulfil:

$$E - E_{1/2} = \frac{RT}{nF} \ln \frac{I_{\lim,c} - I}{I + \left| I_{\lim,a} \right|} \qquad \text{for EC, CE and catalytic processes} \tag{14}$$

where:

$$E_{1/2}^{\mathrm{EC}} = E^{0'} + \frac{RT}{nF} \ln \frac{1+K}{K + \delta_r / \delta} \tag{15}$$

$$E_{1/2}^{\mathrm{CE}} = E^{0'} + \frac{RT}{nF} \ln \frac{1+K\,\delta_r / \delta}{1+K} \tag{16}$$

$$E_{1/2}^{\mathrm{cat}} = E^{0'} \tag{17}$$

$I_{\lim,c}$ and $I_{\lim,a}$ are the cathodic and anodic limiting current of the corresponding mechanism:

$$I_{\lim,c}^{\mathrm{EC}} = I_d \left(c_{\mathrm{A}}^* \right) \tag{18}$$

$$I_{\lim,c}^{\mathrm{CE}} = I_d \left(\zeta^* \right) \tag{19}$$

$$I_{\lim,c}^{\mathrm{cat}} = nFAD\zeta^* / (1+K)\,\delta_r \tag{20}$$

$$I_{\lim,a}^{\mathrm{EC}} = -\frac{K}{\left(K + \delta_r / \delta \right)} I_d \left(c_{\mathrm{A}}^* \right) \zeta^* / c_{\mathrm{A}}^* \tag{21}$$

$$I_{\lim,a}^{\mathrm{CE}} = -I_d \left(\zeta^* \right) c_{\mathrm{D}}^* / \zeta^* \tag{22}$$

$$I_{\lim,a}^{\mathrm{cat}} = -KnFAD\zeta^* / (1+K)\,\delta_r \tag{23}$$

2.4.1. Particular cases

a) True steady state

If the electrode radius r_0 is restricted to the interval $\sqrt{D/\kappa}/10 \le r_0 \le \sqrt{\pi Dt}/20$, the spherical reaction layer thickness δ_r (Eq. (7)) remains unaltered, whereas the spherical diffusion layer thickness δ, given by Eq. (8), simplifies to $\delta^{micro} = r_0$. In this particular case, the half wave potentials corresponding to EC and CE mechanism become independent of time (see Eqs. (15)-(16)).

b) Planar electrode

In planar diffusion $r_0 \to \infty$ and therefore, the reaction and the diffusion layer thicknesses, δ_r, and δ, given by Eqs. (7) and (8), simplify to $\delta_r^{plan} = \sqrt{D/\kappa}$ and $\delta^{plan} = \sqrt{\pi Dt}$, respectively. Note that in this case the half wave potentials of EC and CE processes behave as that deduced by Koutecký applying the reaction layer model [11]. Moreover, note that in planar electrodes an independent of time response can not be reached.

3. DIFFERENTIAL PULSE VOLTAMMETRY

We can establish a direct relationship between the derivative response dI/dE and the differential pulse voltammetry (DPV). DPV is a double pulse potential technique in which two potential pulses of amplitude E_1 and E_2 and length t_1 and t_2, respectively, with $t_1 >> t_2$, being $\Delta E = E_2 - E_1$, are applied to an electrode with the potential scanned in the negative direction ($\Delta E < 0$) or in the positive direction ($\Delta E > 0$) in such a way that a delay between each pair of pulses is introduced in order for the equilibrium to be re-established [6]. In this potentiostatic technique the difference $I_{\mathrm{DPV}} = I_2(t_1 + t_2) - I_1(t_1)$ is plotted vs. E_1.

As is well known, the response ($I_{\mathrm{DPV}}/\Delta E$) vs. E_1 can be considered practically identical to the derivative of the $I-E$ curve (derivative voltammetry) for a reversible E process under the right conditions [4-8]. This criterion can be generalised to the three mechanisms we are considering in this paper, EC, CE and catalytic, once we have demonstrated (see above) that their *I-E* responses can be linearized as that corresponding to an E reversible process.

Then, if we consider a sufficiently small difference between the applied potentials ΔE (which has been established in the bibliography as $\Delta E << RT/nF$ [4, 5, 7], we can take an approximation of the response $I_{\mathrm{DPV}} - E_1$ to the derivative response $dI/dE - E$:

$$I_{\mathrm{DPV}} \simeq \Delta E \times \frac{dI}{dE} \quad \text{if} \quad \Delta E << \frac{RT}{nF} \tag{24}$$

Analysing the peak heights, we find that $(I_{\mathrm{DV}})_{peak}$ coincides with $(I_{\mathrm{DPV}})_{peak}$, with an error of less than 5%, if $\Delta E < 1.6\,RT/nF$. On the other hand, on comparing the peak potentials we find that the difference between both techniques is less than 5% if $\Delta E < 10$ mV, according to the above references [12, 13]. However, on plotting I_{DPV} vs. $(E_1 + E_2)/2$, this last restriction disappears, since in this case the DPV peak potential coincides with that obtained for DV.

Therefore, the $dI/dE - E$ responses applicable to the DPV technique can be easily deduced for EC, CE and catalytic processes under these conditions, from the derivative of Eqs. (3), (9) and (11), respectively.

3.1. EC mechanism

From Eq. (3) and (24) we obtain:

$$I_{\mathrm{DPV}}^{\mathrm{EC}} \simeq -\Delta E \frac{nF}{RT} I_d\left(c_{\mathrm{A}}^*\right) \frac{\left(K\zeta^*/c_{\mathrm{A}}^* + \left(K + \delta_r/\delta\right)\right)(1+K)e^{\eta}}{\left(1 + K + \left(K + \delta_r/\delta\right)e^{\eta}\right)^2} \tag{25}$$

The peak parameters are as follow:

$$E_{peak}^{\mathrm{EC}} = E_{1/2}^{\mathrm{EC}} \tag{26}$$

$$\left(I_{\mathrm{DPV}}^{\mathrm{EC}}\right)_{peak} = -\Delta E \frac{nF}{4RT} I_d\left(c_{\mathrm{A}}^*\right)\left(1+\frac{K\zeta^*/c_{\mathrm{A}}^*}{K+\delta_r/\delta}\right) \tag{27}$$

$$\Delta E_{p/2} \simeq 90 \text{ mV} \tag{28}$$

where $\Delta E_{p/2}$ is the peak half width.

Note that if we define:

$$\eta_{1/2}^{\mathrm{EC}} = \frac{nF}{RT}\left(E - E_{1/2}^{\mathrm{EC}}\right) \tag{29}$$

Eq. (25) can be rewritten as:

$$I_{\mathrm{DPV}}^{\mathrm{EC}} \simeq -\Delta E \frac{nF}{RT} I_d\left(c_{\mathrm{A}}^*\right)\left(1+\frac{K\zeta^*/c_{\mathrm{A}}^*}{K+\delta_r/\delta}\right)\frac{1}{4\cosh^2\left(\eta_{1/2}^{\mathrm{EC}}/2\right)} \tag{30}$$

From Eqs. (26) and (27) it can be seen that both the peak potential E_{peak}^{EC} (Eq. (26)) and the peak height $(I_{\mathrm{DPV}}^{\mathrm{EC}})_{peak}$ $(= I_{\mathrm{DPV}}^{\mathrm{EC}}(E = E_{peak}^{\mathrm{EC}})$, Eq. (27)) are in relation to the kinetic parameters (κ $(= k_1 + k_2)$) and to the equilibrium constant (K) of the homogeneous chemical reaction. However, note that in the most usual case in which $\zeta^* = 0$, the peak height coincides with that obtained for a simple charge transfer process ($(I_{\mathrm{DPV}}^{\mathrm{EC}})_{peak}(\zeta^* = 0) = -\Delta E(nF/4RT) I_d(c_{\mathrm{A}}^*)$) and it does not give any information about the homogeneous kinetic.

Taking into account Eq. (27), we can rewrite Eq. (30) as:

$$\frac{I_{\mathrm{DPV}}^{\mathrm{EC}}}{\left(I_{\mathrm{DPV}}^{\mathrm{EC}}\right)_{peak}} = \frac{1}{\cosh^2\left(\eta_{1/2}^{\mathrm{EC}}/2\right)} \tag{31}$$

3.2. CE mechanism

From Eq. (9) and (24) we obtain:

$$I_{\mathrm{DPV}}^{\mathrm{CE}} \simeq -\Delta E \frac{nF}{RT} I_d\left(\zeta^*\right)\frac{\left(1+\left(1+K\delta_r/\delta\right)c_{\mathrm{D}}^*/\zeta^*\right)\left(1+K\right)e^{\eta}}{\left(1+K\delta_r/\delta+\left(1+K\right)e^{\eta}\right)^2} \tag{32}$$

The peak parameters are as follows:

$$E_{peak}^{\mathrm{CE}} = E_{1/2}^{\mathrm{CE}} \tag{33}$$

$$\left(I_{\mathrm{DPV}}^{\mathrm{CE}}\right)_{peak} = -\Delta E \frac{nF}{4RT} I_d\left(\zeta^*\right)\left(\frac{c_{\mathrm{D}}^*}{\zeta^*}+\frac{1}{1+K\delta_r/\delta}\right) \tag{34}$$

$$\Delta E_{p/2} \simeq 90 \text{ mV} \tag{35}$$

Introducing

$$\eta_{1/2}^{\mathrm{CE}} = \frac{nF}{RT}\left(E - E_{1/2}^{\mathrm{CE}}\right) \tag{36}$$

Eq. (32) can be rewritten as:

$$I_{\mathrm{DPV}}^{\mathrm{CE}} \simeq -\Delta E \frac{nF}{RT} I_d\left(\zeta^*\right)\left(\frac{c_{\mathrm{D}}^*}{\zeta^*}+\frac{1}{1+K\delta_r/\delta}\right)\frac{1}{4\cosh^2\left(\eta_{1/2}^{\mathrm{CE}}/2\right)} \tag{37}$$

From Eqs. (33) and (34) it can be seen that both the peak potential E_{peak}^{CE} (Eq. (33)) and the peak height $(I_{\mathrm{DPV}}^{\mathrm{CE}})_{peak}$ $(=I_{\mathrm{DPV}}^{\mathrm{CE}}(E=E_{peak}^{\mathrm{CE}})$, Eq. (34)) are in relation to the kinetic parameters (κ $(=k_1+k_2)$) and to the equilibrium constant (K) of the homogeneous reaction.

Taking into account Eq. (34), we can rewrite Eq. (37) as:

$$\frac{I_{\mathrm{DPV}}^{\mathrm{CE}}}{\left(I_{\mathrm{DPV}}^{\mathrm{CE}}\right)_{peak}}=\frac{1}{\cosh^2\left(\eta_{1/2}^{\mathrm{CE}}/2\right)} \tag{38}$$

3.3. Catalytic mechanism

From Eq. (11) and (24) we obtain:

$$I_{\mathrm{DPV}}^{\mathrm{cat}} \simeq -\Delta E \frac{nF}{RT}\frac{nFAD\zeta^*}{\delta_r}\frac{1}{4\cosh^2\left(\eta/2\right)} \tag{39}$$

The peak parameters are as follows:

$$E_{peak}^{\mathrm{cat}} = E_{1/2}^{\mathrm{cat}} \tag{40}$$

$$\left(I_{\mathrm{DPV}}^{\mathrm{cat}}\right)_{peak} = -\Delta E \frac{nF}{4RT}\frac{nFAD\zeta^*}{\delta_r} \tag{41}$$

$$\Delta E_{p/2} \simeq 90 \text{ mV} \tag{42}$$

and, as can be seen, the peak half width value is identical for these three mechanisms (see also Eqs. (28) and (35)), indicating that χ $(=\kappa t)$ is sufficiently high or that ξ $(=\sqrt{Dt}/r_0)$ takes the convenient value to satisfy the kinetic steady state.

From these equations it can be seen that only the peak height (Eq. (41)) is in direct relation to the kinetic parameters (κ $(=k_1+k_2)$) of the homogeneous reaction.

Taking into account Eq. (41), we can rewrite Eq. (39) as:

$$\frac{I_{\mathrm{DPV}}^{\mathrm{cat}}}{\left(I_{\mathrm{DPV}}^{\mathrm{cat}}\right)_{peak}}=\frac{1}{\cosh^2\left(\eta/2\right)} \tag{43}$$

4. RESULTS AND DISCUSSION

In Fig. 1 we have studied the different behaviour of the three mechanisms EC (Fig. 1a), CE (Fig. 1b) and catalytic (Fig. 1c) with the variation of χ $(=\kappa t)$ in order to emphasize that this technique allows us to discriminate them. The figure shows the normalized differential pulse

voltammograms for different values of $\sqrt{\chi}$ $(=\sqrt{\kappa t})$ obtained for these three mechanisms. It can be seen that the peak potentials of the $I_{DPV}-E$ curves are shifted towards more positive and more negative values with an increasing of χ for EC and CE processes, respectively, whereas in the case of the catalytic mechanism, the peak potentials remain at the formal potential value. On the other hand, the peak height is independent of the homogeneous kinetic in the case of the EC mechanism (in the more usual case for which $\zeta^* = 0$), whereas it increases with χ $(=\kappa t)$ for the CE and catalytic processes, with this increase being more noticeable in the last case.

Taking all of these results into account, the criteria to discriminate between EC, CE and catalytic processes analyzing the influence of the kinetic constants χ $(=\kappa t)$ in $I_{DPV}-E$ curves, which can be easily deduced from Eqs. (26),(27), (33), (34), (40) and (41), are summed up in Table 1.

Table 1. Effects on peak potential and peak height of EC, CE and catalytic processes when the dimensionless chemical rate constant χ $(=\kappa t)$ increases.

Mechanisms	**Peak potential**	**Peak height**
EC	moves towards more positive potentials	does not vary $(=nF/4RT)$
CE	moves towards more negative potentials	increases
Catalytic	does not vary $(=E^{0'})$	notoriously increases

Hence, it is possible to characterize EC, CE and catalytic mechanisms by changing the dimensionless rate constants, which can be done by modifying the experimental time pulse t or by modifying the experimental conditions (such as pH in the case of the reduction of an acid in a buffered solution or the concentration of ligand in the case of the reduction of a metal complex) if the chemical reaction is of pseudo-first order [2].

In Fig. 2 the responses of EC and CE mechanisms in DPV have been compared with those obtained for catalytic and E mechanisms. In this figure the $\left|I_{DPV}/\Delta E\right|/4\pi r_0 nFDc^*$ vs. $E-E^{0'}$ curves (where $c^* = c_A^*$ for EC mechanism and $c^* = \zeta^*$ for CE and catalytic mechanisms), corresponding to EC, CE (solid lines in Figs. 2a and 2b respectively) and catalytic (dashed lines) mechanisms have been plotted for different values of ξ $(=\sqrt{Dt}/r_0)$. Thus, Eqs. (30), (37) and (39) can be rewritten, respectively, as:

$$\frac{I_{DPV}^{EC}}{4\pi r_0 nFDc_A^*} \simeq -\Delta E \frac{nF}{RT}\frac{r_0}{\delta}\left(1+\frac{K\zeta^*/c_A^*}{K+\delta_r/\delta}\right)\frac{1}{4\cosh^2\left(\eta_{1/2}^{EC}/2\right)} \tag{44}$$

$$\frac{I_{DPV}^{CE}}{4\pi r_0 nFD\zeta^*} \simeq -\Delta E \frac{nF}{RT}\frac{r_0}{\delta}\left(\frac{c_D^*}{\zeta^*}+\frac{1}{1+K\delta_r/\delta}\right)\frac{1}{4\cosh^2\left(\eta_{1/2}^{CE}/2\right)} \tag{45}$$

$$\frac{I_{DPV}^{cat}}{4\pi r_0 nFD\zeta^*} \simeq -\Delta E \frac{nF}{RT}\frac{r_0}{\delta_r}\frac{1}{4\cosh^2\left(\eta/2\right)} \tag{46}$$

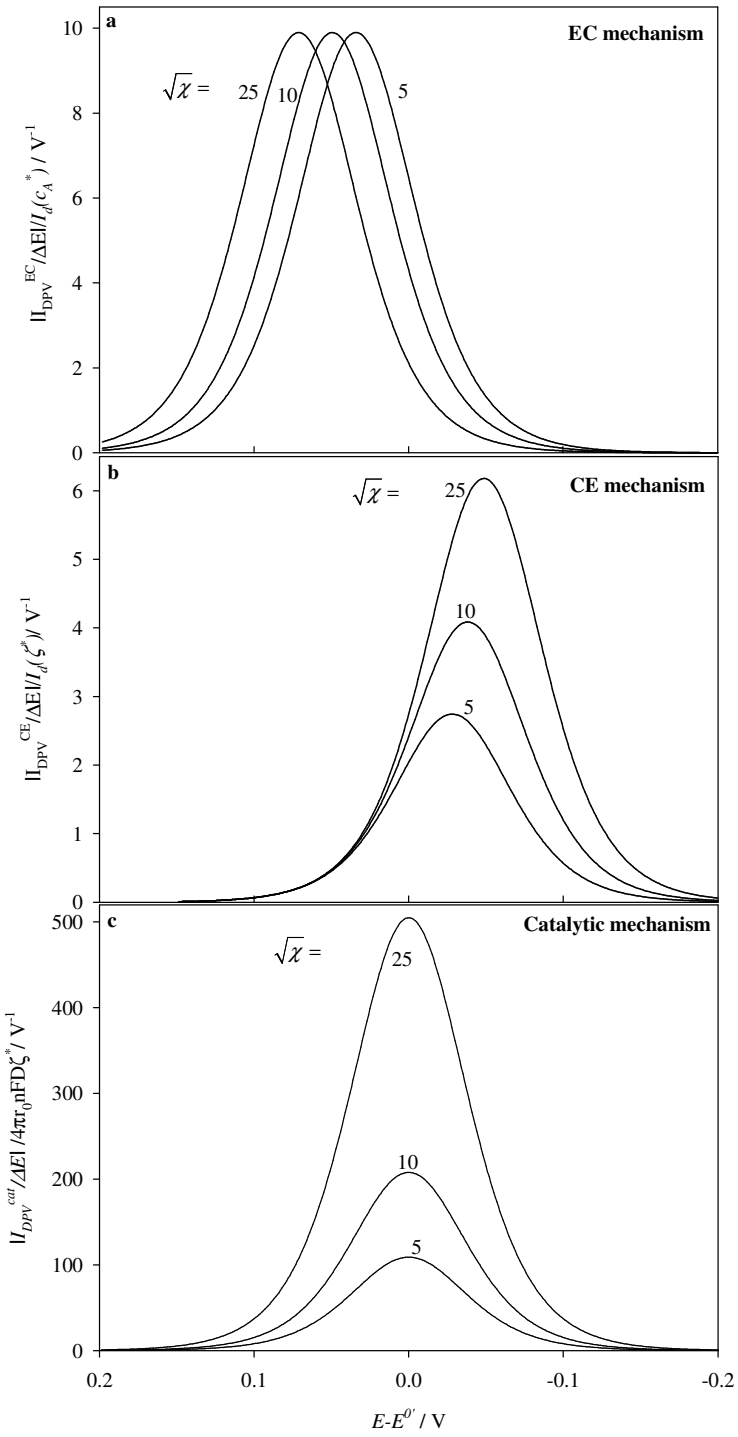

Figure 1. $\left|I_{\mathrm{DPV}}^{\mathrm{EC}}/\Delta E\right|/I_d(c_{\mathrm{A}}^*)$ (1a, Eq. (30)), $\left|I_{\mathrm{DPV}}^{\mathrm{CE}}/\Delta E\right|/I_d(\zeta^*)$ (1b, Eq. (37)) and $\left|I_{\mathrm{DPV}}^{\mathrm{cat}}/\Delta E\right|/4\pi r_0 nFD\zeta^*$ (1c, Eq. (39)) vs. $E-E^{0'}$ curves for several values of $\sqrt{\chi}$ ($=\sqrt{\kappa t}$). EC mechanism (1a): $K=0$, $\zeta^*=0$; CE mechanism (1b): $K=10$, $c_{\mathrm{D}}^*=0$; catalytic mechanism (1c): $K=0$. $\xi=1$ ($r_0=3.2\times10^{-3}$ cm, considering $t=1$ s and $D=10^{-5}$ cm^2 s^{-1}). Values of $\sqrt{\chi}$ are on the curves.

As can be seen in this figure, a decrease of the electrode radius r_0 (i.e., an increase of $\xi (= \sqrt{Dt} / r_0)$) gives a decrease of the peak heights in all the cases. However, whereas the peak potential of the catalytic curves remains independent of the sphericity of the electrode, and is equal to the formal potential $E^{0'}$ (see Eq. (17)), the corresponding to EC or CE mechanisms moves away from $E^{0'}$ towards more negative and more positive potentials, respectively, as r_0 decreases, i.e., ξ increases (Eqs. (15) and (16)), in such a way that for high values of the sphericity electrode (see curves for $\xi = 100$), the curves obtained for these mechanisms are almost superimposable with that obtained for the catalytic process (dashed line) and also practically coincide (with an error of less than 10%) with the one corresponding to a simple charge transfer process (E mechanism, see the dotted lines) under stationary conditions, i.e. when r_0 decreases. This fact indicates that, in this case ($\sqrt{\chi} = 10$), the homogeneous kinetic of the chemical reaction cannot be studied with sphericity values of $\xi \geq 100 (= 10\sqrt{\chi}$ [14, 15]) since it has been masked or immobilized. The movement of the peak potential for EC and CE mechanisms with the variation of ξ can also be used as a criterion in order to identify and discriminate these three mechanisms.

Thus, taking all of these results into account, the criteria to discriminate between EC, CE and catalytic processes analyzing the influence of the sphericity of the electrode $\xi (= \sqrt{Dt} / r_0)$ in $I_{\mathrm{DPV}} - E$ curves, which can be easily deduced from Eqs. (26),(27), (33), (34), (40) and (41), are summed up in Table 2.

Table 2. Effects on peak potential and peak height of EC, CE and catalytic processes when the sphericity of the electrode $\xi (= \sqrt{Dt} / r_0)$ increases.

Mechanisms	**Peak potential**	**Peak height**
EC	moves towards more negative potentials	slightly decreases
CE	moves towards more positive potentials	decreases
Catalytic	does not vary $(= E^{0'})$	notorously decreases

It is interesting to note that Eqs. (30), (37) and (39), for EC, CE and catalytic mechanisms, respectively, are explicit expressions and such that it is possible to analytically deduce the peak parameters (Eqs. (26)-(27), (33)-(34) and (40)-(41)), from which the homogeneous kinetic rate constants can be obtained. Thus, in the case of an EC process we can deduce $\kappa (= k_1 + k_2)$ from the peak potential (Eq. (26)):

$$\kappa^{\mathrm{EC}} = D \left[\frac{\theta_{peak}^{\mathrm{EC}}}{\delta \left(1 + K - K\theta_{peak}^{\mathrm{EC}} \right)} - \frac{1}{r_0} \right]^2 \tag{47}$$

with:

$$\theta_{peak}^{\mathrm{EC}} = \exp \left[\frac{nF}{RT} \left(E_{peak}^{\mathrm{EC}} - E^{0'} \right) \right] \tag{48}$$

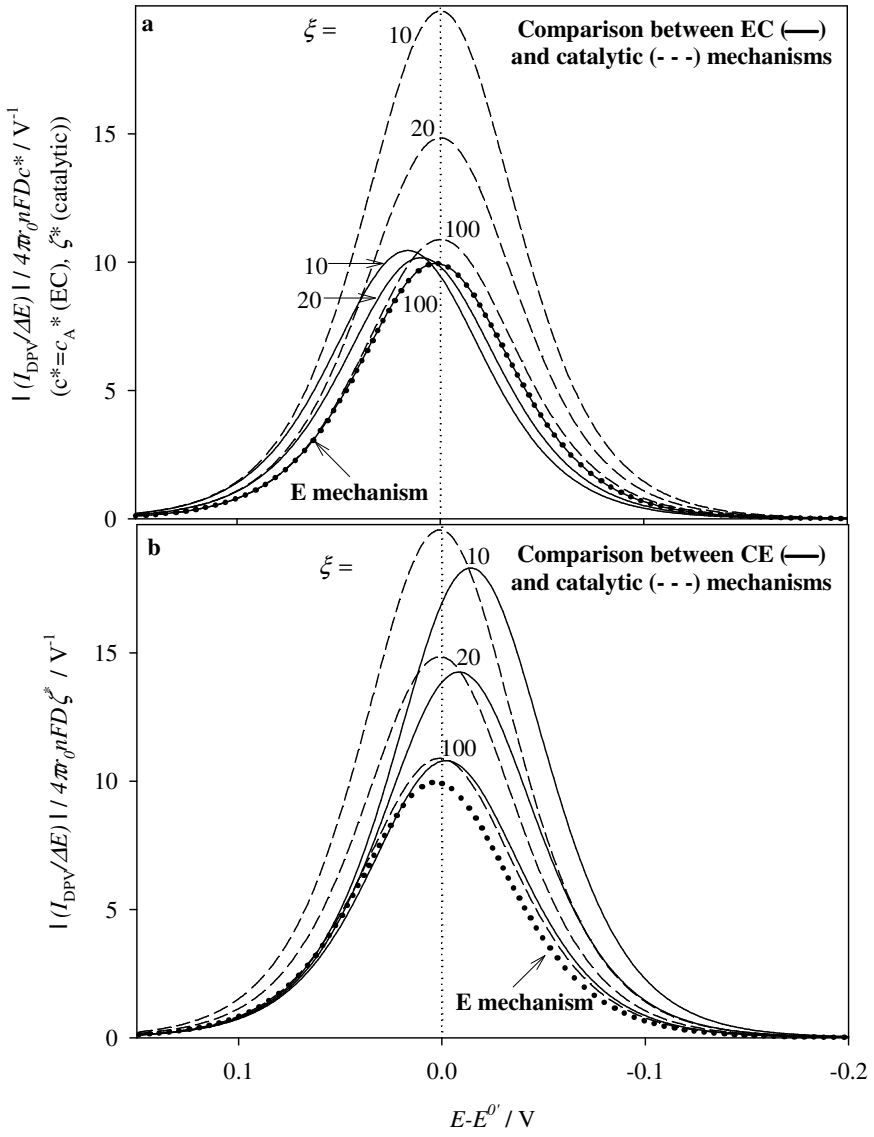

Figure 2. $\left|I_{\mathrm{DPV}}/\Delta E\right|/4\pi r_0 nFDc^*$ vs. $E-E^{0'}$ curves ($c^*=c_{\mathrm{A}}^*$ for EC mechanism and $c^*=\zeta^*$ for CE and catalytic mechanisms) for several values of ξ corresponding to EC (solid lines in 2a, Eq. (44)), CE (solid lines in 2b, Eq. (45)) and catalytic (dashed lines, Eq. (46)) mechanisms. The dotted line is obtained for an E mechanism under stationary conditions. $\sqrt{\chi}=10$. EC mechanism: $K=0$, $\zeta^*=0$. CE mechanism: $K=10$, $c_{\mathrm{D}}^*=0$. Catalytic mechanism: $K=0$. Values of ξ are on the curves. Considering $t=1$ s and $D=10^{-5}$ cm^2 s^{-1} the corresponding r_0 values (in cm) from minor to major ξ values are: 3.2×10^{-4}, 1.6×10^{-4} and 3.2×10^{-5}.

The kinetic constants, κ $(=k_1+k_2)$, for a CE process can be obtained from the peak potential (Eq.(33)),

$$\kappa^{\mathrm{CE}} = D\left[\frac{K}{\delta\left(\left(1+K\right)\theta_{peak}^{\mathrm{CE}}-1\right)}-\frac{1}{r_0}\right]^2 \tag{49}$$

with:

$$\theta_{peak}^{\mathrm{CE}} = \exp\left[\frac{nF}{RT}\left(E_{peak}^{\mathrm{CE}}-E^{0'}\right)\right] \tag{50}$$

or from the peak height (Eq. (34)):

$$\kappa^{\mathrm{CE}} = D\left[\frac{K}{\delta}\frac{\left(4RT/nF\right)\dfrac{\left|\left(I_{DPV}^{\mathrm{CE}}\right)_{peak}\right|}{I_d\left(\zeta^*\right)\Delta\mathrm{E}}-c_{\mathrm{D}}^*/\zeta^*}{1-\left(4RT/nF\right)\dfrac{\left|\left(I_{DPV}^{\mathrm{CE}}\right)_{peak}\right|}{I_d\left(\zeta^*\right)\Delta\mathrm{E}}+c_{\mathrm{D}}^*/\zeta^*}-\frac{1}{r_0}\right]^2 \tag{51}$$

In the case of a catalytic process we can deduce κ from the peak height (Eq. (41)), obtaining:

$$\kappa^{\mathrm{cat}} = D\left(\frac{4RT}{nF}\frac{1}{nFAD\zeta^*}\frac{\left|\left(I_{DPV}^{\mathrm{cat}}\right)_{peak}\right|}{\Delta E}-\frac{1}{r_0}\right)^2 \tag{52}$$

Moreover, as is shown in the following figures, we can propose working curves to obtain the homogeneous kinetic rate constants from the peak potentials (Fig. 3) and the peak heights (Figs. 4 and 5), which, as has been shown, depend on the value of the rate constants and the equilibrium constant of the chemical reaction. In comparison with dc procedures for the determination of the rate constants, DPV reveals a much more accurate due to that the peak is scarcely affected by no desired influences as are double layer and ohmic drop effects.

In Fig. 3 we have plotted the variation of the peak potential with $\sqrt{\chi}$ ($=\sqrt{\kappa t}$) for EC (Fig. 3a, Eq. (26)) and CE (Fig. 3b, Eq. (33)) mechanisms, for different values of the sphericity of the electrode, ξ ($=\sqrt{Dt}/r_0$). From this figure it can be seen that the peak potential shifts towards more positive (Fig. 3a) and more negative (Fig. 3b) values when χ increases or ξ decreases. The figure shows that the peak potentials become independent of the homogeneous kinetic parameters when the electrode sphericity ξ increases and χ decreases. Thus, the curve for $\xi = 100$ differs by less than 10% from that corresponding to an E mechanism (dotted line) if $\sqrt{\chi} < 10$.

Fig. 4 shows the variation of the normalized peak height with $\sqrt{\chi}$ for a CE mechanism (Eq. (34)) for different values of the equilibrium constant K. From this figure it can be seen that, for this mechanism, the peak height always increases with $\sqrt{\chi}$ and decreases with K. Moreover, the determination of $\sqrt{\chi}$ is clearly more accurate with lower values of the equilibrium constant. Thus, once the peak height has been calculated, and the equilibrium constant K is known, we can obtain $\sqrt{\chi}$ from the *x*-axis of the corresponding curve.

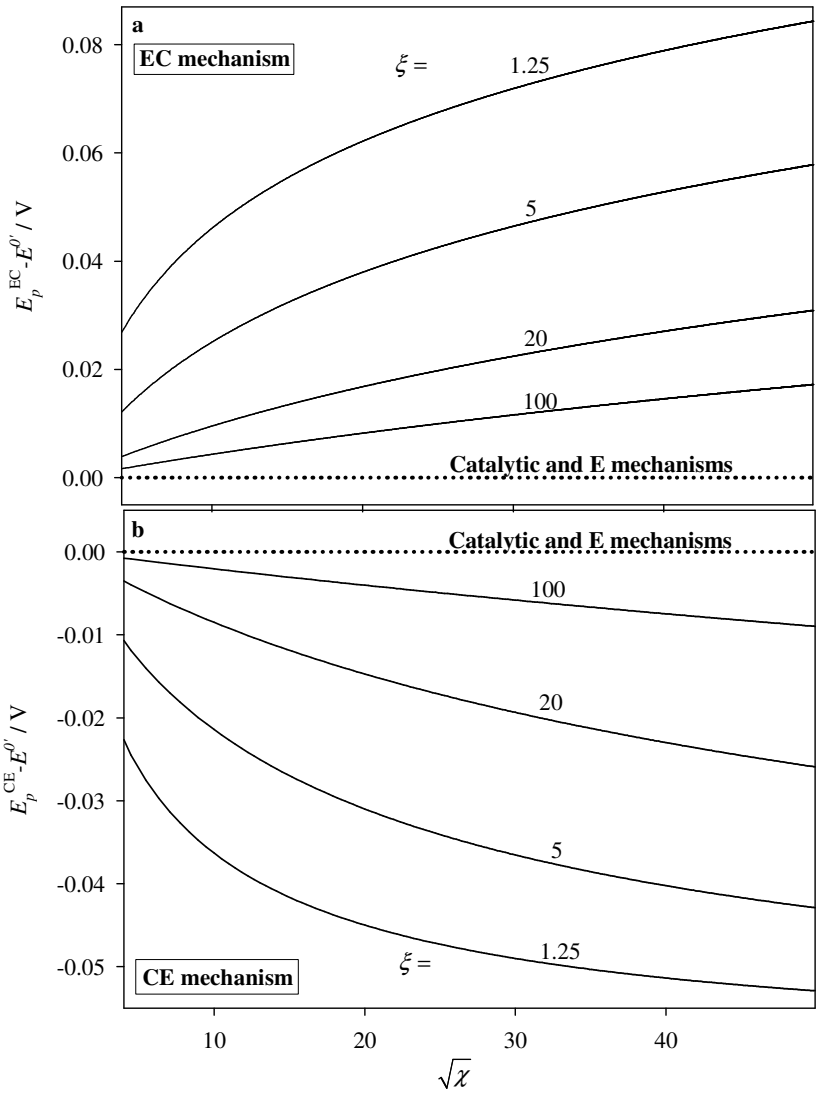

Figure 3. Variation of the peak potential with $\sqrt{\chi}$ for EC (3a, Eq. (26)) and CE (3b, Eq. (33)) mechanisms for different values of the sphericity of the electrode, ξ. $K = 0$, $\zeta^* = 0$ (EC mechanism, 3a); $K = 10$, $c_D^* = 0$ (CE mechanism, 3b). Values of ξ are on the curves. Considering $t = 1$ s and $D = 10^{-5}$ cm^2 s^{-1}, the corresponding r_0 values (in cm), from minor to major ξ values, are: 2.5×10^{-3}, 6.3×10^{-4}, 1.6×10^{-4}, 3.2×10^{-5}.

In Fig. 5 we can see the variation of the normalized peak height of a catalytic mechanism with $\sqrt{\chi}$ (Eq. (41)) for different values of the sphericity of the electrode, ξ. From this figure it can be seen that the peak height always increases with $\sqrt{\chi}$ and decreases with ξ. Moreover, the determination of $\sqrt{\chi}$ is clearly more accurate with lower values of the electrode sphericity. Thus, in the case of a catalytic process it is possible to obtain $\sqrt{\chi}$ from the *x*-axis of the curve corresponding to the appropriate ξ value.

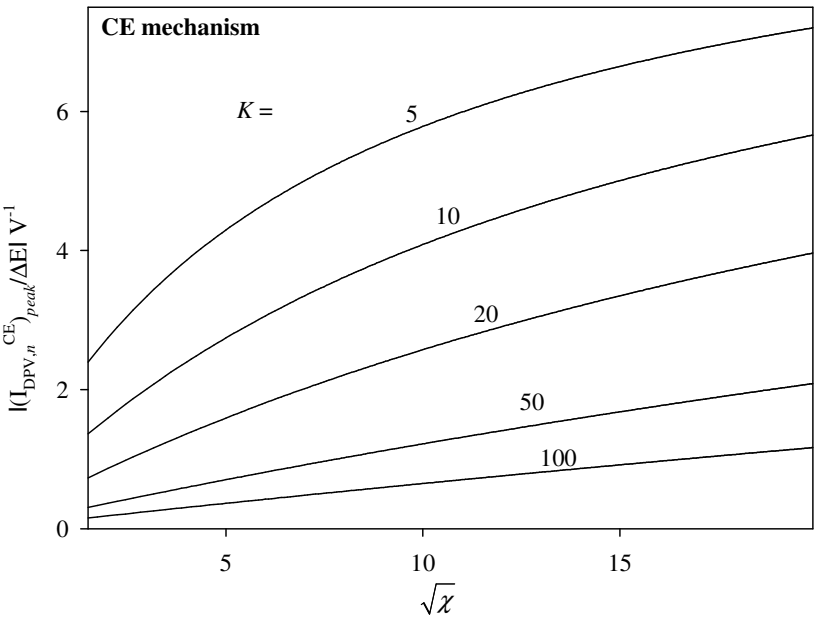

Figure 4. Variation of the normalized peak height of a CE mechanism $\left|(I_{\mathrm{DPV}}^{\mathrm{CE}})_{peak}/\Delta E\right|/I_d(\zeta^*)$ with $\sqrt{\chi}$ (Eq. (34)) for different values of the equilibrium constant K (see Eq. (34)). $\xi = 1$ ($r_0 = 3.2\times10^{-3}$ cm considering $t = 1$ s and $D = 10^{-5}$ cm^2 s^{-1}), $c_{\mathrm{D}}^* = 0$. Values of K are on the curves.

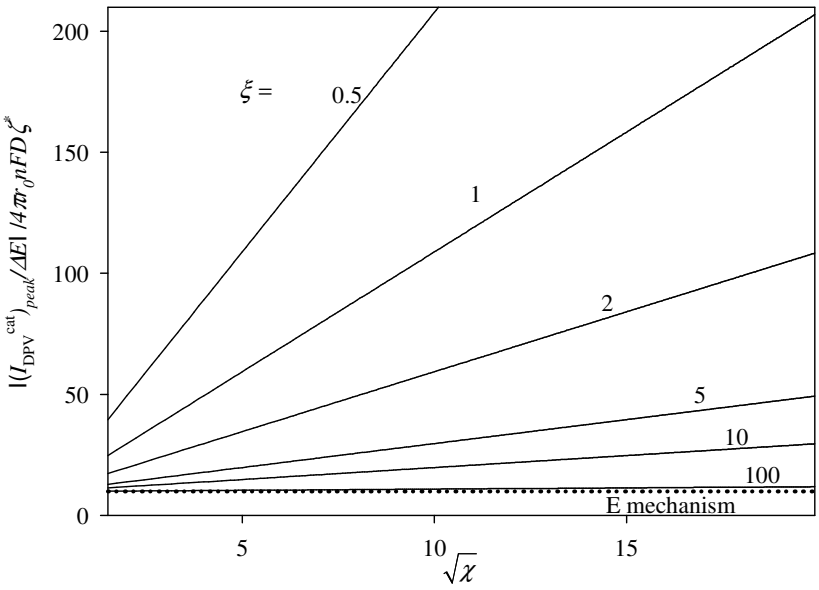

Figure 5. Variation of the normalized peak height of a catalytic mechanism ($\left|(I_{\mathrm{DPV}}^{\mathrm{cat}})_{peak}/\Delta E\right|/4\pi r_0 nFD\zeta^*$) with $\sqrt{\chi}$ (Eq. (41)) for different values of the sphericity of the electrode. Values of ξ are on the curves. Considering $t = 1$ s and $D = 10^{-5}$ cm^2 s^{-1}, the corresponding r_0 values (in cm), from minor to major ξ values, are: 6.3×10^{-3}, 3.2×10^{-3}, 1.6×10^{-3}, 6.3×10^{-4}, 3.2×10^{-4}, 3.2×10^{-5}.

Note that the dependence of the normalized peak height, $\left|(I_{\mathrm{DPV}}^{\mathrm{cat}})_{peak}/\Delta E\right|/4\pi r_0 nFD\zeta^*$, with $\sqrt{\chi}$ is linear, as can be deduced from Eq. (41). In this case, it is interesting to note that the dependence of $(I_{\mathrm{DPV}}^{\mathrm{cat}})_{peak}/\Delta E$ with ξ and χ is "fictitious", in such a way that the true dependence is with r_0 and κ, since, as has been pointed out, this response is independent of time under kinetic steady state conditions.

5. CONCLUSIONS

- We have deduced the voltammetric $I-E$ response corresponding to an EC mechanism, and also the derivative voltammetric responses, $dI/dE-E$, for EC, CE and catalytic mechanisms which are also applicable to differential pulse voltammetry ($I_{\mathrm{DPV}}-E$) when $\Delta E << RT/nF$. This study has been carried out analytically, from the explicit equations obtained under the kinetic steady state approximation with the additional condition of considering a purely diffusive behaviour for ζ, c_{A} and c_{D}.
- The $I-E$ curves of EC, CE and catalytic mechanisms can be linearized in a formally identical way to the corresponding to an E reversible process, being the half wave potential $E_{1/2}$ dependent on the chemical rate constant κ of each process and on the electrode radius in the case of EC and CE processes.
- We have found criteria to discriminate between EC, CE and catalytic processes based on the influence of the dimensionless chemical rate constants ($\chi=\kappa t$) and the electrode radius ($\xi=\sqrt{Dt}/r_0$) in $I_{\mathrm{DPV}}-E$ curves. The results are summarized in Tables 1 and 2.
- We have given easy analytical expressions to determine the kinetic constants of the chemical reaction from the peak parameters (peak potentials and/or peak heights) of the $I_{\mathrm{DPV}}-E$ curves. Moreover, we have also plotted working curves in order to calculate these kinetic constants of the chemical reactions.

6. Appendix

The mass transport to/from the electrode surface when a constant potential, E, is applied to a spherical electrode of radius r_0 is described by the following differential equation system and boundary value problem:

$$\left.\begin{aligned}
&\hat{\delta}_{\mathrm{A}}c_{\mathrm{A}}(r,t)=0 && \text{(a)}\\
&\hat{\delta}_{\mathrm{B}}c_{\mathrm{B}}(r,t)=-k_1c_{\mathrm{B}}(r,t)+k_2c_{\mathrm{C}}(r,t) && \text{(b)}\\
&\hat{\delta}_{\mathrm{C}}c_{\mathrm{C}}(r,t)=k_1c_{\mathrm{B}}(r,t)-k_2c_{\mathrm{C}}(r,t) && \text{(c)}
\end{aligned}\right\} \qquad \text{(A1)}$$

where:

$$\hat{\delta}_i=\frac{\partial}{\partial t}-D_i\left(\frac{\partial^2}{\partial r^2}+\frac{2}{r}\frac{\partial}{\partial r}\right) \qquad \text{(A2)}$$

$$\left.\begin{array}{l} t=0,\ r\geq r_0 \\ t>0,\ r\to\infty \end{array}\right\} \qquad c_{\mathrm{A}}(r,t)=c_{\mathrm{A}}^{*},\ c_{\mathrm{B}}(r,t)=c_{\mathrm{B}}^{*},\ c_{\mathrm{C}}(r,t)=c_{\mathrm{C}}^{*} \tag{A3}$$

$$\left.\begin{array}{l} t>0,\ r=r_0 \end{array}\right\} \qquad D_{\mathrm{A}}\left(\frac{\partial c_{\mathrm{A}}(r,t)}{\partial r}\right)_{r=r_0}=-D_{\mathrm{B}}\left(\frac{\partial c_{\mathrm{B}}(r,t)}{\partial r}\right)_{r=r_0} \tag{A4}$$

$$\left(\frac{\partial c_{\mathrm{C}}(r,t)}{\partial r}\right)_{r=r_0}=0 \tag{A5}$$

$$c_{\mathrm{A}}(r_0,t)=e^{\eta}c_{\mathrm{B}}(r_0,t) \tag{A6}$$

where:

$$\eta=\frac{nF}{RT}\left(E-E^{0'}\right) \tag{A7}$$

and E is the applied potential. The current obtained is given by:

$$I=nFAD_{\mathrm{A}}\left(\frac{\partial c_{\mathrm{A}}(r,t)}{\partial r}\right)_{r=r_0}=-nFAD_{\mathrm{B}}\left(\frac{\partial c_{\mathrm{B}}(r,t)}{\partial r}\right)_{r=r_0} \tag{A8}$$

F and *A* having their usual electrochemical meanings.

With the introduction of variables ζ and ϕ, defined as [2]:

$$\zeta(r,t)=c_{\mathrm{B}}(r,t)+c_{\mathrm{C}}(r,t) \tag{A9}$$

$$\phi(r,t)=c_{\mathrm{B}}(r,t)-Kc_{\mathrm{C}}(r,t) \tag{A10}$$

where $\phi(r,t)$ measures the perturbation of the chemical equilibrium (see Eq. (1)), and considering equidiffusivity conditions, which set that $D_{\mathrm{B}}=D_{\mathrm{C}}=D_{\mathrm{D}}=D$, the equation system (A1) and the boundary value problem (A3)-(A6) simplify to:

$$\left.\begin{array}{ll} \hat{\delta}c_{\mathrm{A}}(r,t)=0 & \text{(a)} \\ \hat{\delta}\zeta(r,t)=0 & \text{(b)} \\ \hat{\delta}\phi(r,t)=-\kappa\phi(r,t) & \text{(c)} \end{array}\right\} \tag{A11}$$

$$\left.\begin{array}{l} t=0,\ r\geq r_0 \\ t>0,\ r\to\infty \end{array}\right\} \qquad c_{\mathrm{A}}(r,t)=c_{\mathrm{A}}^{*},\quad \zeta(r,t)=\zeta^{*}=c_{\mathrm{B}}^{*}+c_{\mathrm{C}}^{*},\quad \phi(r,t)=0 \tag{A12}$$

$$\left.\begin{array}{l} t>0,\ r=r_0 \end{array}\right\} \qquad \left(\frac{\partial c_{\mathrm{A}}(r,t)}{\partial r}\right)_{r=r_0}=-\left(\frac{\partial \zeta(r,t)}{\partial r}\right)_{r=r_0} \tag{A13}$$

$$\left(\frac{\partial \zeta(r,t)}{\partial r}\right)_{r=r_0}=\left(\frac{\partial \phi(r,t)}{\partial r}\right)_{r=r_0} \tag{A14}$$

$$(1+K)c_{\mathrm{A}}(r_0,t) = e^{\eta}\left[K\zeta(r_0,t)+\phi(r_0,t)\right] \tag{A15}$$

with the current (Eq. (A8)) given by:

$$I = nFAD\left(\frac{\partial c_{\mathrm{A}}(r,t)}{\partial r}\right)_{r=r_0} = -nFAD\left(\frac{\partial \zeta(r,t)}{\partial r}\right)_{r=r_0} \tag{A16}$$

The kinetic steady state approximation only affects the variable ϕ (Eq. (A10)) and supposes that the perturbation of the chemical equilibrium is independent of time, i. e., $\partial\phi(r,t)/\partial t = 0$ [2, 3]. Under this condition, the solution for the variable ϕ in Eq. (A11)b is immediately obtained,

$$\phi(r) = \frac{r_0}{r}\phi(r_0)\exp\left[-\sqrt{\frac{\kappa}{D}}(r-r_0)\right] \tag{A17}$$

in such a way that taking into account Eqs. (A14) and (A16) also, we can write:

$$\frac{I}{nFAD} = -\left(\frac{\partial \zeta(r,t)}{\partial r}\right)_{r=r_0} = -\left(\frac{\partial \phi(r)}{\partial r}\right)_{r=r_0} = \frac{\phi(r_0)}{\delta_r} \tag{A18}$$

with

$$\delta_r = \left(\frac{1}{r_0}+\sqrt{\frac{\kappa}{D}}\right)^{-1} = \frac{r_0\sqrt{D}}{\sqrt{D}+r_0\sqrt{\kappa}} \tag{A19}$$

We now introduce an additional approximation which has been shown in a recent paper to be fundamental for the general definition and understanding of the spherical reaction and diffusion layers [16].

In this approximation, the variable ϕ (Eq. (A10)) fulfils the kinetic steady state condition ($\partial\phi/\partial t = 0$). In relation to variables c_{A} and ζ, we consider also that $\partial c_{\mathrm{A}}/\partial t \neq 0$ and $\partial\zeta/\partial t \neq 0$, and therefore both variables must verify Eqs. (A11)a and (A11)b. At this point, we simplify this problem by assuming that the solutions of Eqs. (A11)a and (A11)b have the same form as that for species that would only suffer spherical diffusion and would keep independent of time values at the electrode surface [2]. Thus, for any value of the applied potential, *E*, the solutions for c_{A} and ζ have the form:

$$c_{\mathrm{A}}(r,t) = c_{\mathrm{A}}^{*} - \frac{r_0}{r}\left(c_{\mathrm{A}}^{*} - c_{\mathrm{A}}(r_0)\right)erfc\left(\frac{r-r_0}{2\sqrt{Dt}}\right) \tag{A20}$$

$$\zeta(r,t) = \zeta^{*} - \frac{r_0}{r}\left(\zeta^{*} - \zeta(r_0)\right)erfc\left(\frac{r-r_0}{2\sqrt{Dt}}\right) \tag{A21}$$

where $c_{\mathrm{A}}(r_0)$ and $\zeta(r_0)$ are the value of c_{A} and ζ at the electrode surface at any constant E value. From Eqs. (A17) and (A21) the concentration profiles of species B and C can be immediately obtained:

$$c_{\mathrm{B}}(r,t)=\frac{1}{1+K}\left\{K\zeta^{*}-\frac{r_0}{r}\left[K\left(\zeta^{*}-\zeta(r_0)\right)erfc\left(\frac{r-r_0}{2\sqrt{Dt}}\right)-\phi(r_0)\exp\left(-\sqrt{\frac{\kappa}{D}}(r-r_0)\right)\right]\right\} \tag{A22}$$

$$c_{\mathrm{C}}(r,t)=\frac{1}{1+K}\left\{\zeta^{*}-\frac{r_0}{r}\left[\left(\zeta^{*}-\zeta(r_0)\right)erfc\left(\frac{r-r_0}{2\sqrt{Dt}}\right)+\phi(r_0)\exp\left(-\sqrt{\frac{\kappa}{D}}(r-r_0)\right)\right]\right\} \tag{A23}$$

Eqs. (A20) and (A21) fulfil, respectively:

$$\left(\frac{\partial c_{\mathrm{A}}(r,t)}{\partial r}\right)_{r=r_0}=\frac{c_{\mathrm{A}}^{*}-c_{\mathrm{A}}(r_0)}{\delta} \tag{A24}$$

$$\left(\frac{\partial \zeta(r,t)}{\partial r}\right)_{r=r_0}=\frac{\zeta^{*}-\zeta(r_0)}{\delta} \tag{A25}$$

where δ is the diffusion layer thickness:

$$\delta=\left(\frac{1}{r_0}+\frac{1}{\sqrt{\pi Dt}}\right)^{-1} \tag{A26}$$

From Eqs. (A13), (A15), (A18), (A24) and (A25) we obtain:

$$\frac{c_{\mathrm{A}}(r_0)}{c_{\mathrm{A}}^{*}}=\frac{\left[K\left(1+\zeta^{*}/c_{\mathrm{A}}^{*}\right)+\delta_r/\delta\right]e^{\eta}}{1+K+\left(K+\delta_r/\delta\right)e^{\eta}} \tag{A27}$$

$$\frac{\zeta(r_0)}{c_{\mathrm{A}}^{*}}=\frac{(1+K)\left(1+\zeta^{*}/c_{\mathrm{A}}^{*}\right)+e^{\eta}\left(\delta_r/\delta\right)\zeta^{*}/c_{\mathrm{A}}^{*}}{1+K+\left(K+\delta_r/\delta\right)e^{\eta}} \tag{A28}$$

$$\frac{\phi(r_0)}{c_{\mathrm{A}}^{*}}=\frac{\delta_r}{\delta}\frac{1+K-Ke^{\eta}\,\zeta^{*}/c_{\mathrm{A}}^{*}}{1+K+\left(K+\delta_r/\delta\right)e^{\eta}} \tag{A29}$$

and taking into account Eqs. (A9) and (A10) we deduce the surface concentrations of species B and C:

$$\frac{c_{\mathrm{B}}(r_0)}{c_{\mathrm{A}}^{*}}=\frac{\delta_r/\delta+K\left(1+\zeta^{*}/c_{\mathrm{A}}^{*}\right)}{1+K+\left(K+\delta_r/\delta\right)e^{\eta}} \tag{A30}$$

$$\frac{c_{\mathrm{C}}(r_0)}{c_{\mathrm{A}}^{*}}=\frac{1-\delta_r/\delta+\left(1+e^{\eta}\,\delta_r/\delta\right)\zeta^{*}/c_{\mathrm{A}}^{*}}{1+K+\left(K+\delta_r/\delta\right)e^{\eta}} \tag{A31}$$

The concentration profiles of species A, B and C are obtained by introducing Eq. (A27) in Eq. (A20) and Eqs. (A28)-(A29) in Eqs. (A22)-(A23), respectively:

$$\frac{c_{\mathrm{A}}(r,t)}{c_{\mathrm{A}}^{*}}=1-\frac{r_0}{r}\frac{1+K-Ke^{\eta}\zeta^{*}/c_{\mathrm{A}}^{*}}{1+K+\left(K+\delta_r/\delta\right)e^{\eta}}erfc\left(\frac{r-r_0}{2\sqrt{Dt}}\right) \tag{A32}$$

$$\frac{c_{\mathrm{B}}(r,t)}{c_{\mathrm{A}}^{*}}=\frac{1}{1+K}\left\{K\frac{\zeta^{*}}{c_{\mathrm{A}}^{*}}+\frac{r_0}{r}\frac{1+K-Ke^{\eta}\zeta^{*}/c_{\mathrm{A}}^{*}}{1+K+\left(K+\delta_r/\delta\right)e^{\eta}}\times\left[Kerfc\left(\frac{r-r_0}{2\sqrt{Dt}}\right)+\frac{\delta_r}{\delta}\exp\left(-\sqrt{\frac{\kappa}{D}}(r-r_0)\right)\right]\right\} \tag{A33}$$

$$\frac{c_C(r,t)}{c_A^*} = \frac{1}{1+K}\left\{\frac{\zeta^*}{c_A^*} + \frac{r_0}{r}\frac{1+K-Ke^{\eta}\zeta^*/c_A^*}{1+K+(K+\delta_r/\delta)e^{\eta}} \times \left[erfc\left(\frac{r-r_0}{2\sqrt{Dt}}\right) - \frac{\delta_r}{\delta}\exp\left(-\sqrt{\frac{\kappa}{D}}(r-r_0)\right)\right]\right\} \quad \text{(A34)}$$

Finally, from Eq. (A18), and taking into account Eqs. (A24)-(A29), the following expression for the current is obtained:

$$\frac{I^{EC}\delta}{nFADc_A^*} = \frac{1+K-Ke^{\eta}\,\zeta^*/c_A^*}{1+K+e^{\eta}(K+\delta_r/\delta)} \quad \text{(A35)}$$

ACKNOWLEDGEMENTS

The authors greatly appreciate the financial support provided by the Dirección General de Investigación (MEC) (Project Number CTQ2006-12552/BQU) and by the Fundación SENECA (Expedient number 03079/PI/05). Also, I. M. thanks the Ministerio de Educación y Ciencia for the grant received.

References

[1] A. Molina, I. Morales, *J. Electroanal. Chem.* 583 (2005) 193.
[2] A. Molina, I. Morales, M. López-Tenés, *Electrochem. Commun.* 8 (2006) 1062.
[3] I. Morales, A. Molina, *Electrochem. Commun.* 8 (2006) 1453
[4] J. Heyrovský, J. Kuta, *Principles of Polarography*, Academic Press, New York, 1966, Ch. XVII
[5] E.P. Parry, R.A. Osteryoung, *Anal. Chem.* 37 (1965) 1634.
[6] A.J. Bard, L.R. Faulkner, *Electrochemical Methods. Fundamental and Applications*, second ed., Wiley, New York, 2001
[7] A. Molina, J. González, *Electrochem. Commun.* 1 (1999) 477.
[8] J. González, A. Molina, M. López-Tenés, C. Serna, *J. Electrochem. Soc.* 147 (2000) 3429.
[9] Z. Galus, *Fundamentals of Electrochemical Analysis*, second ed., Ellis Horwood, Chichester, 1994.
[10] K.B. Oldham, *J. Electroanal. Chem.* 313 (1991) 3.
[11] J. Koutecký, R. Brdicka, *Coll. Czech. Chem. Commun.* 12 (1947) 337.
[12] M. Vukovic, D. Cukman, V. Pravdic, *J. Electroanal. Chem.* 54 (1974) 209.
[13] M. Vukovic, D. Cukman, V. Pravdic, *J. Electroanal. Chem.* 62 (1975) 387.
[14] J. Koutecký, *Chem. Listy* 47 (1953) 323.
[15] J. Koutecký, *Collection Czech. Chem. Commun.* 18 (1953) 597.
[16] C. Serna, A. Molina, *J. Electroanal. Chem.* 466 (1999) 8.